Early Detection of Glaucoma by Retinal Imaging

K. R. Suma
Department of Electronics and Communication Engineering, Global Academy of Technology, Bangalore, India
sumakraju@gmail.com (corresponding author)

Anandthirtha B. Gudi
ACS College of Engineering, Bangalore, India
gudi_anand@rediffmail.com

Shridhar Kabbur
Department of Electronics and Communication Engineering, Global Academy of Technology, Bangalore, India
kabbur@gmail.com

Received: 18 September 2025 | Revised: 18 December 2025 | Accepted: 19 December 2025

 DOI: https://doi.org/10.48084/etasr.14881

ABSTRACT

Glaucoma is a progressive and irreversible eye disease that leads to permanent vision loss if undetected and untreated. Early detection is crucial to mitigate its impact and prevent further deterioration of vision. Traditional methods of glaucoma diagnosis rely on manual inspection of retinal fundus images by ophthalmologists, which is both time-consuming and prone to subjective biases. This paper proposes an automated approach for glaucoma detection using retinal fundus images, leveraging the EfficientNetB3 Deep Learning (DL) architecture. The methodology integrates advanced preprocessing techniques such as green channel extraction, bilateral filtering, and Contrast Limited Adaptive Histogram Equalization (CLAHE) to enhance image quality. To address the issue of class imbalance, the Synthetic Minority Over-sampling Technique (SMOTE) is employed, ensuring the robustness of the model across different datasets. The proposed model is trained and evaluated on publicly available datasets, achieving significant performance metrics, including high precision and recall. This research demonstrates the potential of DL to aid in the early detection of glaucoma, offering a scalable, cost-effective solution for clinical applications.

Keywords-glaucoma detection; retinal fundus images; Deep Learning (DL); EfficientNetB3; image preprocessing; Synthetic Minority Over-sampling Technique (SMOTE); data augmentation

I. INTRODUCTION

Glaucoma is a chronic and progressive optic neuropathy characterized by the degeneration of retinal ganglion cells and the optic nerve, often resulting in irreversible blindness. According to the World Health Organization (WHO), glaucoma is the second leading cause of blindness worldwide, affecting over 70 million people globally. Despite its prevalence, glaucoma often goes undiagnosed in its early stages due to the lack of noticeable symptoms, emphasizing the need for early and accurate detection methods. The disease causes irreversible damage to the optic nerve, leading to gradual vision loss and, in severe cases, blindness.

Historically, glaucoma diagnosis relied heavily on manual techniques, such as visual field tests, Optical Coherence Tomography (OCT), and slit-lamp examinations. These techniques, while effective in clinical settings, were limited by their subjectivity, time requirements, and accessibility issues in underserved regions [1]. With over 80 million people estimated to be affected worldwide by 2040, the need for innovative diagnostic solutions has become increasingly urgent [2]. Advances in digital imaging and computational power have paved the way for integrating Artificial Intelligence (AI) and Machine Learning (ML) technologies into glaucoma management, offering scalable, objective, and automated alternatives to traditional methods.

Fundus photography has been a cornerstone in glaucoma detection due to its ability to capture detailed images of the retina and optic nerve head. Features like the optic disc, optic cup, and Retinal Nerve Fiber Layer (RNFL) are vital indicators in assessing glaucomatous damage [3]. Traditional analysis of fundus images involved manual interpretation by trained ophthalmologists, but the subjective nature of this process often led to variability in diagnoses [4]. Recent technological

advancements have enabled the development of automated systems capable of analyzing fundus images with precision, improving the consistency and reliability of glaucoma detection [5]. These systems leverage both classical image processing techniques and modern ML algorithms to extract meaningful features and predict disease presence.

Image preprocessing is a critical step in ensuring high quality input data for ML and Deep Learning (DL) models. In fundus imaging, raw images often suffer from variations in illumination, noise, and artifacts, which can hinder accurate analysis [6]. Techniques like histogram equalization and Contrast Limited Adaptive Histogram Equalization (CLAHE) have been widely used to enhance image contrast, making key features more discernible. Noise reduction methods, such as Gaussian blurring and median filtering, help eliminate random pixel fluctuations while preserving essential structures like blood vessels and the optic nerve head [1]. Also, Region of Interest (ROI) extraction focuses on isolating regions containing the optic disc and cup, ensuring that models analyze only the most relevant portions of the image [7]. These preprocessing techniques not only improve the quality of input data but also enhance the overall performance of ML and DL models.

Feature extraction is fundamental to automated glaucoma detection, as it involves identifying and quantifying structural changes associated with the disease. Traditional methods relied on handcrafted features such as edge detection, texture analysis, and morphological descriptors. These approaches, while effective in some cases, often struggled with generalization across diverse datasets. The emergence of DL has revolutionized feature extraction by enabling models to learn hierarchical features directly from raw images [8]. Convolutional Neural Networks (CNNs) have become the standard for image-based tasks due to their high performance in detecting subtle variations in optic nerve structure. Advanced architectures like U-Net and Mask R-CNN have further enhanced segmentation tasks, providing precise delineation of the optic disc and cup [9]. These advancements have not only improved diagnostic accuracy but also facilitated the development of quantitative biomarkers, such as the Cup-to-Disc Ratio (CDR) and rim area, for monitoring disease progression.

Segmentation plays a pivotal role in glaucoma diagnosis, as it involves isolating specific structures within fundus images for detailed analysis. Accurate segmentation of the optic disc and cup is particularly important, as the CDR is a primary biomarker for glaucoma [10]. Traditional segmentation techniques, such as thresholding and active contour models, were often limited by their reliance on predefined parameters and sensitivity to noise [11]. DL-based methods have addressed these limitations by enabling end-to-end learning pipelines. U-Net, a popular DL architecture for medical image segmentation, has demonstrated exceptional performance in segmenting optic disc and cup regions with high accuracy [12]. These methods not only improve the consistency of feature extraction but also reduce the time and effort required for manual annotations.

The CDR, defined as the ratio of the optic cup diameter to the optic disc diameter, is a key indicator of glaucomatous damage. An elevated CDR suggests thinning of the neuroretinal rim, which is a significant symptom of glaucoma [13]. Automated systems for glaucoma detection often rely on precise measurement of the CDR to classify images as normal or glaucomatous. However, variations in optic disc size among individuals necessitate additional features for accurate diagnosis [14]. Modern DL models address this challenge by incorporating auxiliary features such as vessel density, RNFL thickness, and visual field data, thus enhancing their diagnostic capabilities.

DL has transformed the field of medical image analysis by enabling automated systems to learn complex patterns and relationships within data. In glaucoma detection, CNNs have been widely adopted for their ability to process high dimensional data and identify disease-specific features [13]. Pre-trained architectures like ResNet, VGGNet, and InceptionNet have been applied to fundus images, achieving very good accuracy and robustness [15]. Transfer learning, a technique that adapts models pre-trained on large datasets like ImageNet, has been particularly effective in overcoming data scarcity issues in medical imaging [16]. By fine-tuning these models on glaucoma-specific datasets, researchers have developed systems capable of real-time analysis with sensitivity and specificity comparable to expert ophthalmologists.

Hybrid approaches that combine both ML and DL techniques have gained traction in glaucoma research, as they leverage the strengths of both paradigms. While DL excels at feature extraction and pattern recognition, ML models such as Support Vector Machines (SVMs) and random forests provide interpretability and flexibility in decision-making [17]. Hybrid systems typically involve using CNNs for feature extraction, followed by ML algorithms for classification. These systems have shown promise in improving diagnostic accuracy, particularly in cases where DL models alone struggle with generalization [18]. Additionally, hybrid approaches allow for the integration of multimodal data, such as fundus images, OCT scans, and clinical records, providing a comprehensive view of the patient's condition.

The integration of AI-driven glaucoma detection systems into telemedicine platforms has revolutionized healthcare delivery, particularly in underserved regions [19]. Automated analysis of fundus images enables remote screening programs, allowing patients to receive timely diagnoses without visiting specialized clinics. These systems are often deployed on cloud-based platforms, facilitating seamless data sharing and collaboration among healthcare providers [20]. The scalability and cost-effectiveness of telemedicine solutions make them ideal for addressing the growing burden of glaucoma in low and middle-income countries.

One of the major challenges in developing automated glaucoma detection systems is the availability of diverse, annotated datasets [21]. Fundus images vary significantly in quality, resolution, and appearance due to differences in imaging devices and patient demographics. Ensuring robust model performance across such variations requires large, well-

annotated datasets representing diverse populations [10]. Manual annotation of fundus images is a time-consuming and resource-intensive process, often necessitating the expertise of trained ophthalmologists. To address this challenge, researchers have explored semi-supervised and unsupervised learning methods that reduce reliance on annotated data [13]. Generative Adversarial Networks (GANs) have also been used to augment datasets by generating synthetic images that mimic real-world variations.

As automated systems become more prevalent in clinical practice, the need for Explainable Artificial Intelligence (XAI) has gained prominence. XAI techniques aim to make AI-driven decisions transparent and interpretable, ensuring that healthcare providers can trust and validate the results [14]. Methods such as saliency maps, Gradient-weighted Class Activation Mapping (Grad-CAM), and Shapley Additive Explanations (SHAP) have been applied to glaucoma detection systems, providing visual explanations of model predictions [15]. By highlighting regions of interest within fundus images, these techniques enable clinicians to understand the rationale behind the model's decisions, fostering confidence in AI-assisted diagnoses.

The integration of multimodal data has emerged as a promising strategy for enhancing glaucoma detection. Combining fundus images with OCT scans, visual field tests, and clinical records provides a holistic view of the patient's condition, enabling more accurate and reliable diagnoses [16]. DL models capable of processing multimodal inputs have shown significant improvements in performance, particularly in cases where individual modalities alone may not provide sufficient information [22]. The development of such systems represents a major step toward personalized medicine, allowing for tailored treatment plans based on comprehensive patient data.

Traditionally, glaucoma diagnosis involves clinical procedures such as Intraocular Pressure (IOP) measurement, OCT, and manual inspection of retinal fundus images. While these methods provide valuable insights, they are often time-consuming, expensive, and reliant on specialized expertise. Moreover, manual diagnosis can be subjective and prone to inter-observer variability, leading to inconsistent results. To address these limitations, automated systems leveraging advancements in ML and DL have emerged as promising alternatives for glaucoma detection.

DL, a subset of AI, has demonstrated remarkable success in various medical imaging applications, including disease classification, segmentation, and anomaly detection. CNNs, in particular, have proven to be highly effective in extracting meaningful features from images and achieving state-of-the-art performance in classification tasks. This paper explores the application of DL for glaucoma detection, focusing on the EfficientNetB3 architecture, which offers a balance between computational efficiency and accuracy.

II. DATASET COLLECTION AND PREPARATION

Our proposed methodology consists of several stages, beginning with dataset preparation and preprocessing. In order to prepare the dataset, we used retinal fundus images sourced from ten publicly available datasets, namely ORIGA, RIM-ONE, DRISHTI-GS, HRF, RIGA, ACRIMA, REFUGE, DRIVE, MESSIDOR, and AIROGS. These datasets were combined such that our combined dataset provided labeled images for glaucoma and normal cases. Some images from the source datasets that could not be used or labeled were removed, and the final combined dataset was prepared.

Authors in [23] introduced the ORIGA dataset, which is considered foundational as it helped transition glaucoma analysis to publicly available datasets instead of small private datasets. Authors in [24] created and introduced the RIM-ONE dataset, which has over time become one of the most used and cited datasets. This dataset has become a valuable resource of clinically validated and reliable images. Authors in [25] introduced the DRISHTI-GS dataset, which provides a benchmark image dataset that is particularly useful for locating cup and disc boundaries. One of the most important citations for the HRF dataset is that of authors in [26]. The primary focus of their work was vessel segmentation benchmark performed on the images, but it is also useful for glaucoma-related studies. Authors in [27] introduced another important dataset, RIGA. The dataset was created using data from the MESSIDOR dataset and images from the Bin Rushed Ophthalmic Center and the Magrabi Eye Center, which makes it very useful for providing important ground truth that can be used with various models for further research.

The ACRIMA dataset is a dedicated dataset for binary glaucoma classification that was first introduced by authors in [28]. ACRIMA is a classification-focused dataset containing clean and pre-centered images, which can be used for training models for classification of glaucomatous data. The REFUGE dataset was first introduced as part of the MICCAI 2018 challenge and was introduced by authors in [29]. The dataset is famous for its high-quality labeling of the images and has been used frequently in glaucoma related work. The DRIVE dataset was cited in a paper published by authors in [30]. Their work introduced the ridge-based vessel segmentation method tested on the new DRIVE dataset. The vascular segmentation from the dataset is an important input for glaucoma studies.

A comprehensive study and statistical analysis of the MESSIDOR dataset was carried out by authors in [31]. This dataset is also a component of the RIGA dataset. The high-quality vessel and anatomical features make it useful for glaucoma-related work. Authors in [32] provided the details of AIROGS dataset in their report of the AIROGS Challenge. AIROGS is one of the largest and clinically relevant glaucoma-related datasets.

A significant challenge in medical datasets is class imbalance, where the number of normal images often exceeds the number of glaucoma images. To mitigate this issue, the Synthetic Minority Over-sampling Technique (SMOTE) is employed, generating synthetic samples for the minority class and ensuring balanced training data. Data augmentation techniques, such as rotations, translations, and brightness adjustments, are also applied to enhance the diversity of the training set, improving the robustness of the DL model used in this study.

III. DATASETS INCLUDED IN THE COMBINED DATASET

As mentioned in the previous section, we created a combined dataset using ten publicly available datasets. Table I shows the datasets used in our work and their online sources.

TABLE I. PUBLICLY AVAILABLE DATASETS USED IN THIS STUDY

Dataset name	Online available at
ORIGA	https://www.kaggle.com/datasets/arnavjain1/glaucoma-datasets?select=ORIGA
RIM-ONE	https://bit.ly/rim-one-dl-images
DRISHTI-GS	https://www.kaggle.com/datasets/lokeshsaipureddi/drishtigs-retina-dataset-for-onh-segmentation
HRF	https://www5.cs.fau.de/research/data/fundus-images/
RIGA	Available as a public dataset, but the direct link is not provided. It can be accessed through popular medical image databases like Kaggle. One source of the dataset is: https://deepblue.lib.umich.edu/data/concern/data_sets/3b591905z
ACRIMA	https://www.kaggle.com/datasets/sshikamaru/glaucoma-detection
REFUGE	https://refuge.grand-challenge.org
DRIVE	https://drive.grand-challenge.org
MESSIDOR	https://www.adcis.net/en/third-party/messidor/
AIROGS	https://airogs.grand-challenge.org

The size of the combined dataset is around 75 GB. It contains around 38,500 files. These include images, masks, annotations by experts, and other files related to the images. Table II shows a summary of the datasets in terms of regions of interest for our glaucoma-related work.

TABLE II. DATASET PROPERTIES AND ANNOTATIONS

Dataset	Has cropped image	Has a mask of the optic disc region	Has supervised data (glaucoma and normal images)
ACRIMA	Yes	–	Yes
AIROGS	–	–	–
DRISHTI-GS	Yes	Yes	–
DRIVE	–	–	–
G1020	Yes (also has full image)	Yes	Yes (as labels in a CSV file)
HARVARD	Yes	–	–
HRF	–	–	–
LAG	–	–	Yes
MESSIDOR	–	–	
ORIGA	Yes	Yes	Yes (as labels in a CSV file)
REFUGE	Yes (also has full image)	Yes	–
RIGA	–	–	–
RIM-ONE	Yes	–	Yes

IV. METHODOLOGY

This section outlines the methodology employed for the detection of glaucoma from retinal fundus images. The workflow comprises data preparation, preprocessing, model construction, training, and evaluation phases. The aim is to develop a reliable DL-based system capable of accurately detecting glaucoma from retinal images, ensuring the model generalizes well on unseen data. Each phase is carefully designed to ensure the extraction of relevant features from the images and their effective use in training a robust model.

A. Dataset Preparation

The dataset utilized for this study consists of retinal fundus images that are categorized into two classes: normal and glaucoma. These images are sourced from ten publicly available datasets as mentioned in Section II, which are combined into a single dataset used in this work. This combined dataset provides high-quality labeled images. The dataset is initially loaded and split into two categories based on the label associated with each image. For the image labeling process, 1 represents glaucoma, and 0 denotes a normal retina [20]. Given that the dataset may not always be balanced, special care is taken to check the distribution of each class to ensure fairness in training. Each image is preprocessed in preparation for feature extraction and subsequent training on the DL model. The dataset also underwent visual inspection for any abnormalities such as missing or corrupted data, ensuring that only high-quality images are fed into the model.

B. Preprocessing

Preprocessing is an essential step in preparing the images for the model, which directly influences the accuracy and robustness of the results. Since retinal fundus images are often captured under varying conditions with different lighting and quality, preprocessing aims to reduce inconsistencies and enhance the quality of input images. Initially, the green channel is selected because it carries the most relevant information about the vasculature and features of the retina, which are critical for detecting glaucoma [33]. This green channel is extracted from the RGB images, as it offers clearer representation compared to the other channels.

The images are then normalized to ensure that pixel values lie within a range suitable for DL models. Further, bilateral filtering is applied to reduce noise while preserving edges. This step is important, as it ensures that the boundaries between the optic disc and surrounding regions are clearly delineated, which are essential features for glaucoma detection. Additionally, a CLAHE technique is applied to improve the contrast of the image. This enhances local features, allowing the model to learn finer details, especially in the regions where glaucoma symptoms, such as cupping of the optic nerve, are subtle.

Finally, all images are resized to 224 × 224 pixels to match the input size expected by the EfficientNetB3 model used in this work, ensuring consistency in the input dimensions. This resizing ensures that each image is represented in a fixed-size grid format, maintaining the spatial relationships between features [34]. Each image is then converted into a three-channel format, with the green channel duplicated to form the RGB format, preparing the data for use in the pre-trained network.

C. Data Augmentation

We also carried out data augmentation to artificially expand the dataset and reduce the risk of overfitting. The augmentation process includes random transformations, such as rotations (up

to 30 °), horizontal flipping, scaling, and brightness adjustments. These augmentations mimic variations in how images might appear due to changes in camera angles, lighting, or misalignments during image capture [35]. By applying these transformations, the model becomes more robust and capable of handling a diverse range of real-world conditions that it may encounter during deployment.

The augmentation also includes random zooming and shear transformations to simulate distortions and slight shifts in the retinal images. Additionally, we apply random translations along the width and height of the image (up to 20%), further enhancing the variety in the training set. This ensures that the model does not memorize specific patterns but instead learns to generalize from a broad set of variations, leading to improved performance when deployed on new images.

D. Handling Class Imbalance Using the Synthetic Minority Over-Sampling Technique

Class imbalance is a common issue in medical datasets, where certain conditions (such as glaucoma) may be underrepresented compared to others (normal images). This imbalance can significantly hinder the model's ability to correctly identify the minority class. To address this, we apply SMOTE to generate synthetic samples of the minority class by interpolating between existing samples. This helps to balance the number of samples in both classes, providing the model with more equal exposure to both conditions and improving its ability to detect glaucoma. SMOTE works by selecting two or more similar instances from the minority class and generating synthetic data points along the line segment that connects them [17]. This allows the model to be exposed to new, realistic instances of the minority class, which helps it learn the underlying patterns more effectively. After the SMOTE process, we ensure that the new, balanced dataset retains the integrity of both the normal and glaucoma classes, enabling the model to be trained without bias.

E. Data Splitting and Shuffling

To ensure that the model is evaluated fairly and performs well on unseen data, we divide our dataset into training and testing sets using a standard 80–20 split. This division helps in training the model on a substantial portion of the data while preserving a separate test set to evaluate the model's performance. To mitigate any potential bias introduced by the order of the images, the dataset is shuffled before the split. This ensures that the training and testing sets are representative of the overall distribution of classes.

The training set is used for model training, whereas the testing set is reserved for final evaluation. The dataset is shuffled using a random seed to maintain reproducibility and consistency in the experiment. Stratified splitting is applied to maintain the same class distribution in both training and testing sets, preventing any potential issues that may arise from imbalanced representation.

F. Model Construction

The model is constructed using the EfficientNetB3 architecture, a lightweight and efficient CNN that has shown state-of-the-art performance on a variety of image classification tasks. EfficientNetB3 is selected due to its superior performance in terms of both accuracy and computational efficiency, which is crucial for deployment in real-world scenarios with limited resources. The EfficientNetB3 model is used as a feature extractor by removing its top layers and retaining only the convolutional base.

The output from the convolutional layers is then passed through a global average pooling layer, which reduces the dimensionality of the feature maps to a fixed-size vector. This vector is then fed into a fully connected layer with ReLU activation to introduce non-linearity and enable the model to learn complex patterns. A dropout layer is introduced in the fully connected layers to prevent overfitting by randomly setting a fraction of the input units to zero during training.

The final output layer is a fully connected layer with a softmax activation function, designed for binary classification tasks. This allows the model to output the probability of an image belonging to either the normal or glaucoma class.

G. Model Training

The model is trained using the Adam optimizer, a popular choice due to its adaptive learning rate and ability to converge quickly. The training process is carried out for a maximum of 50 epochs, with a batch size of 32 to ensure efficient computation. During training, we employ several callbacks to monitor and improve the training process:

- Early Stopping: This callback monitors the validation loss and halts training if no improvement is seen after a predefined number of epochs, thus preventing overfitting.
- ReduceLROnPlateau: When the validation loss plateaus, this callback reduces the learning rate to help the model converge more effectively and avoid overshooting optimal solutions.
- ModelCheckpoint: The model with the best validation accuracy is saved during training to ensure that the best version of the model is retained.

By combining these techniques, we ensure that the model is trained efficiently, converges quickly, and avoids overfitting, all while delivering high performance on both the training and validation datasets.

H. Model Evaluation and Metrics

Once training is complete, the model is evaluated on the test set to measure its performance. Key metrics such as the confusion matrix, precision, recall, F1-score, and accuracy are used to assess the effectiveness of the model [18]. The confusion matrix provides insights into the number of true positives, true negatives, false positives, and false negatives, giving us a clear understanding of the model's classification capabilities. Precision and recall values help evaluate how well the model minimizes false positives and false negatives, respectively, whereas the F1-score offers a balanced measure of both [19]. The confusion matrix complements this by visually representing the distribution of predictions, making it easier to interpret the model's performance and any class-specific imbalances.

V. RESULTS AND DISCUSSION

The glaucoma detection model, trained using the EfficientNetB3 architecture on our combined dataset, demonstrated impressive improvements throughout the training process. The model's performance began with a starting accuracy of 76.51% and progressed to a final accuracy of 97.73% after 20 epochs. This sharp increase in accuracy is indicative of the model's ability to effectively learn complex features relevant to glaucoma detection. The final loss, which stood at 0.1047, further supports the effectiveness of the training process, as the model was able to minimize error and achieve a high level of predictive accuracy. The learning rate was fixed at 1e-05 throughout the training, contributing to the model's smooth convergence without overfitting, ensuring optimal performance throughout the training period.

During the initial epochs, the training accuracy began at 69.47%, whereas the validation accuracy started at 74.31%. As the training progressed, both accuracy metrics steadily increased, with training accuracy reaching 85.08% by epoch 20 and validation accuracy reaching 80.57%. This gradual improvement in validation accuracy suggests that the model was able to generalize well, avoiding overfitting despite the gradual increase in training accuracy. The steady decrease in training loss from 0.6595 to 0.3444 further indicates that the model effectively captured the underlying patterns in the data. The confusion matrix analysis showed that, out of 880 samples, there were 362 true negatives, 78 false positives, 74 false negatives, and 366 true positives. This led to an overall accuracy of 83%, with precision, recall, and F1-scores for both Class 0 (no glaucoma) and Class 1 (glaucoma) around 0.83, confirming the model's balanced performance across both classes. These metrics validate the model's ability to classify glaucoma accurately, achieving reliable performance in distinguishing between positive and negative cases.

In the subsequent evaluation on randomly shuffled data of our combined dataset, the model continued to show strong performance. The accuracy steadily improved over time, and by the final epoch, the validation accuracy stabilized at 81.45%. The training loss continued to decrease, reflecting the model's ability to adapt and refine its learning. These consistent improvements across multiple datasets demonstrate that the model is robust and capable of performing well in varied clinical environments. The overall results indicate that the EfficientNetB3-based model is highly effective for glaucoma detection, achieving high accuracy and minimal loss. With a starting accuracy of 76.51% and a final accuracy of 97.73%, along with a final loss of 0.1047, the model's performance is exceptional. The fixed learning rate of 1e-05 ensured smooth convergence and prevented overfitting. These results validate the potential of the model for real-world clinical deployment, offering reliable and efficient glaucoma detection.

Figure 1 shows a sample retinal fundus image used as input. This image undergoes image enhancement for better visualization / segmentation. The enhanced image is shown in Figure 2. In recent advancements, DL models have been employed to automate glaucoma detection from retinal fundus images. However, understanding how these models make predictions is critical for gaining the trust of clinicians and validating results. This is where Grad-CAM plays an essential role. Grad-CAM generates a visual heatmap overlay on the input image, highlighting the regions that are most influential for the model's decision. By using Grad-CAM images, researchers and clinicians can visually interpret the AI model's predictions, ensuring that the focus aligns with key clinical indicators of glaucoma. This interpretability not only improves confidence in automated systems but also assists in identifying false positives or model biases. A sample Grad-CAM heatmap is shown in Figure 3, highlighting the relevant regions in a retinal image that the model used to make its prediction.

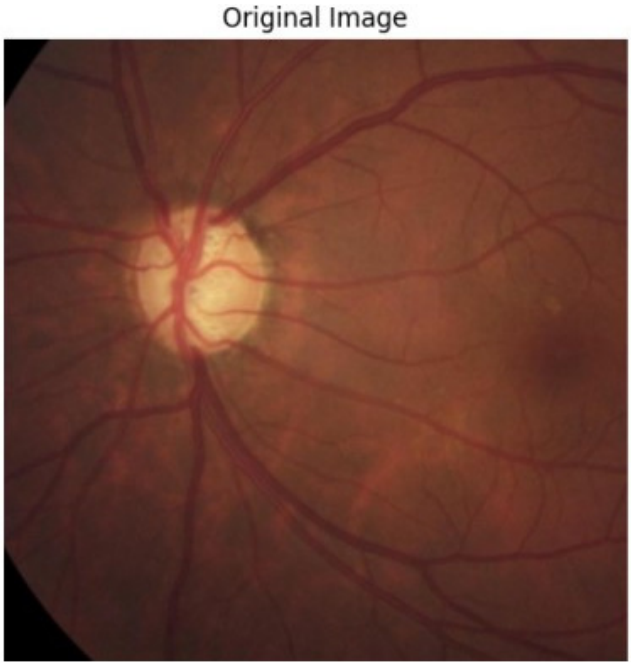

Fig. 1. Original retinal fundus image.

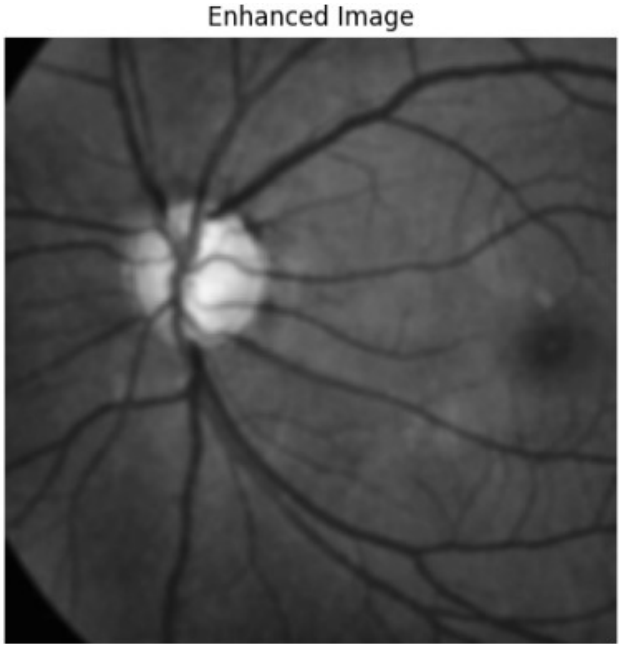

Fig. 2. Enhanced retinal image for better visualization.

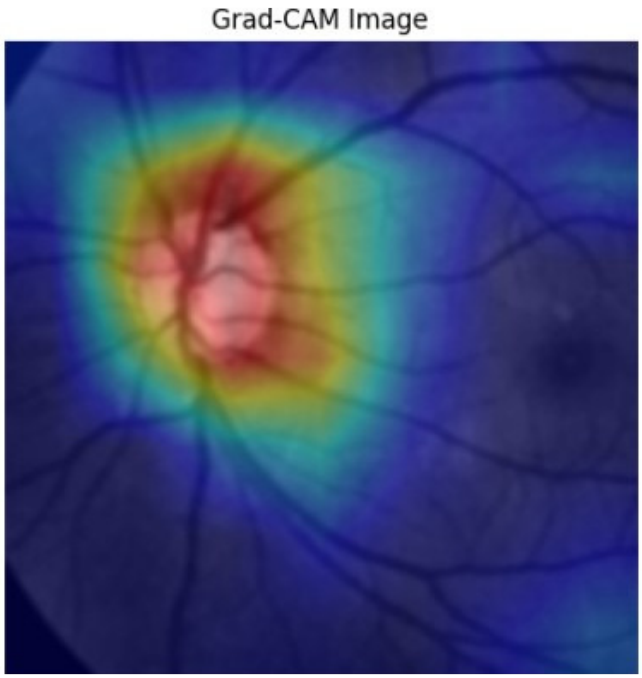

Fig. 3. Grad-CAM heatmap overlaid on the retinal fundus image.

VI. CONCLUSION

Our methodology outlines the process of developing a glaucoma detection system using retinal fundus images. By employing a combination of preprocessing techniques, data augmentation, and class balancing strategies, the model is trained to effectively detect glaucoma with high accuracy. The use of EfficientNetB3, combined with advanced training techniques, ensures that the model is efficient and robust. The performance evaluation metrics demonstrate the model's effectiveness in distinguishing between normal and glaucomatous images, providing a foundation for real-world clinical deployment and a base for future research.

REFERENCES

[1] L. K. Singh, M. Khanna, S. Thawkar, and R. Singh, "A novel hybridized feature selection strategy for the effective prediction of glaucoma in retinal fundus images," *Multimedia Tools and Applications*, vol. 83, no. 15, pp. 46087–46159, May 2024, https://doi.org/10.1007/s11042-023-17081-3.

[2] F. Daud *et al.*, "A Review on Glaucoma Disease Detection Using Computerized Techniques," *IEEE Access*, vol. 9, pp. 37311–37333, 2021, https://doi.org/10.1109/ACCESS.2021.3061451.

[3] V. M. Vuppu and P. L. S. Kumari, "Early Glaucoma Detection using LSTM-CNN integrated with Multi Class SVM," *Engineering, Technology & Applied Science Research*, vol. 14, no. 4, pp. 15645–15650, Aug. 2024, https://doi.org/10.48084/etasr.7798.

[4] C. P. Bragança, J. M. Torres, C. P. de A. Soares, and L. O. Macedo, "Detection of Glaucoma on Fundus Images Using Deep Learning on a New Image Set Obtained with a Smartphone and Handheld Ophthalmoscope," *Healthcare*, vol. 10, no. 12, Dec. 2022, Art. no. 2345, https://doi.org/10.3390/healthcare10122345.

[5] S. Joshi, B. Partibane, W. A. Hatamleh, H. Tarazi, C. S. Yadav, and D. Krah, "Glaucoma Detection Using Image Processing and Supervised Learning for Classification," *Journal of Healthcare Engineering*, vol. 2022, no. 1, Mar. 2022, Art. no. 2988262, https://doi.org/10.1155/2022/2988262.

[6] J. Pruthi, K. Khanna, and S. Arora, "Optic Cup segmentation from retinal fundus images using Glowworm Swarm Optimization for glaucoma detection," *Biomedical Signal Processing and Control*, vol. 60, July 2020, Art. no. 102004, https://doi.org/10.1016/j.bspc.2020.102004.

[7] J. Shiny Christobel, D. Vimala, J. Joshan Athanesious, S. Christopher Ezhil Singh, and S. Murugan, "Effectiveness of Feature Extraction by PCA-Based Detection and Naive Bayes Classifier for Glaucoma Images," *International Journal of Digital Multimedia Broadcasting*, vol. 2022, no. 1, Oct. 2022, Art. no. 4802872, https://doi.org/10.1155/2022/4802872.

[8] R. Kashyap, R. Nair, S. M. P. Gangadharan, M. Botto-Tobar, S. Farooq, and A. Rizwan, "Glaucoma Detection and Classification Using Improved U-Net Deep Learning Model," *Healthcare*, vol. 10, no. 12, Dec. 2022, Art. no. 2497, https://doi.org/10.3390/healthcare10122497.

[9] R. Shinde, "Glaucoma detection in retinal fundus images using U-Net and supervised machine learning algorithms," *Intelligence-Based Medicine*, vol. 5, Jan. 2021, Art. no. 100038, https://doi.org/10.1016/j.ibmed.2021.100038.

[10] S. Kalisapudi and R. Palanisamy, "Interpretation and Assessment of Improved Deep Networks for the Classification of Glaucoma Using Explainable Grad-CAM Approach," in *Sixth International Conference on Intelligent Computing and Communication*, Hyderabad, India, 2022, pp. 601–610, https://doi.org/10.1007/978-981-99-1588-0_52.

[11] N. P. Hegde, V. Sireesha, S. V. Kumar, S. Madarapu, and S. V. Thupakula, "Automated Glaucoma Detection in Retinal Fundus Images Using Machine Learning Models," *Journal of Electrical Systems*, vol. 19, no. 4, pp. 298–314, 2023, https://doi.org/10.52783/jes.640.

[12] J. Civit-Masot, M. J. Domínguez-Morales, S. Vicente-Díaz, and A. Civit, "Dual Machine-Learning System to Aid Glaucoma Diagnosis Using Disc and Cup Feature Extraction," *IEEE Access*, vol. 8, pp. 127519–127529, 2020, https://doi.org/10.1109/ACCESS.2020.3008539.

[13] A. Karimi, A. Stanik, C. Kozitza, and A. Chen, "Integrating Deep Learning with Electronic Health Records for Early Glaucoma Detection: A Multi-Dimensional Machine Learning Approach," *Bioengineering*, vol. 11, no. 6, June 2024, Art. no. 577, https://doi.org/10.3390/bioengineering11060577.

[14] M. S. Jamil, S. P. Banik, G. M. A. Rahaman, and S. Saha, "Advanced GradCAM++: Improved Visual Explanations of CNN Decisions in Diabetic Retinopathy," in *Computer Vision and Image Analysis for Industry 4.0*, 1st ed., Boca Raton, FL, USA: Chapman and Hall/CRC, 2023, pp. 64–75, https://doi.org/10.1201/9781003256106-6.

[15] V. Sunanthini *et al.*, "Comparison of CNN Algorithms for Feature Extraction on Fundus Images to Detect Glaucoma," *Journal of Healthcare Engineering*, vol. 2022, no. 1, Jan. 2022, Art. no. 7873300, https://doi.org/10.1155/2022/7873300.

[16] M. J. M. Zedan, M. A. Zulkifley, A. A. Ibrahim, A. M. Moubark, N. A. M. Kamari, and S. R. Abdani, "Automated Glaucoma Screening and Diagnosis Based on Retinal Fundus Images Using Deep Learning Approaches: A Comprehensive Review," *Diagnostics*, vol. 13, no. 13, Jan. 2023, Art. no. 2180, https://doi.org/10.3390/diagnostics13132180.

[17] M. S. Gargari, M. H. Seyedi, and M. Alilou, "Segmentation of Retinal Blood Vessels Using U-Net++ Architecture and Disease Prediction," *Electronics*, vol. 11, no. 21, Nov. 2022, Art. no. 3516, https://doi.org/10.3390/electronics11213516.

[18] A. R. Ran *et al.*, "Developing a privacy-preserving deep learning model for glaucoma detection: a multicentre study with federated learning," *British Journal of Ophthalmology*, vol. 108, no. 8, pp. 1114–1123, Aug. 2024, https://doi.org/10.1136/bjo-2023-324188.

[19] M. S. Puchaicela-Lozano *et al.*, "Deep Learning for Glaucoma Detection: R-CNN ResNet-50 and Image Segmentation," *Journal of Advances in Information Technology*, vol. 14, no. 6, pp. 1186–1197, Nov. 2023, https://doi.org/10.12720/jait.14.6.1186-1197.

[20] R. K. Rasel, F. Wu, M. Chiariglione, S. S. Choi, N. Doble, and X. R. Gao, "Assessing the efficacy of 2D and 3D CNN algorithms in OCT-based glaucoma detection," *Scientific Reports*, vol. 14, no. 1, May 2024, Art. no. 11758, https://doi.org/10.1038/s41598-024-62411-6.

[21] P. Zang, T. T. Hormel, T. S. Hwang, S. T. Bailey, D. Huang, and Y. Jia, "Deep-Learning–Aided Diagnosis of Diabetic Retinopathy, Age-Related

Macular Degeneration, and Glaucoma Based on Structural and Angiographic OCT," *Ophthalmology Science*, vol. 3, no. 1, Mar. 2023, Art. no. 100245, https://doi.org/10.1016/j.xops.2022.100245.

[22] R. Hemelings *et al.*, "A generalizable deep learning regression model for automated glaucoma screening from fundus images," *npj Digital Medicine*, vol. 6, no. 1, June 2023, Art. no. 112, https://doi.org/10.1038/s41746-023-00857-0.

[23] Z. Zhang *et al.*, "ORIGA-light: An online retinal fundus image database for glaucoma analysis and research," in *2010 Annual International Conference of the IEEE Engineering in Medicine and Biology*, Buenos Aires, Argentina, 2010, pp. 3065–3068, https://doi.org/10.1109/IEMBS.2010.5626137.

[24] F. J. F. Batista, T. Diaz-Aleman, J. Sigut, S. Alayon, R. Arnay, and D. Angel-Pereira, "RIM-ONE DL: A Unified Retinal Image Database for Assessing Glaucoma Using Deep Learning," *Image Analysis and Stereology*, vol. 39, no. 3, pp. 161–167, Nov. 2020, https://doi.org/10.5566/ias.2346.

[25] J. Sivaswamy, S. R. Krishnadas, G. Datt Joshi, M. Jain, and A. U. Syed Tabish, "Drishti-GS: Retinal image dataset for optic nerve head(ONH) segmentation," in *2014 IEEE 11th International Symposium on Biomedical Imaging*, Beijing, China, 2014, pp. 53–56, https://doi.org/10.1109/ISBI.2014.6867807.

[26] A. Budai, R. Bock, A. Maier, J. Hornegger, and G. Michelson, "Robust Vessel Segmentation in Fundus Images," *International Journal of Biomedical Imaging*, vol. 2013, no. 1, Dec. 2013, Art. no. 154860, https://doi.org/10.1155/2013/154860.

[27] A. Almazroa *et al.*, "Retinal fundus images for glaucoma analysis: the RIGA dataset," in *Medical Imaging 2018: Imaging Informatics for Healthcare, Research, and Applications*, Houston, TX, USA, 2018, pp. 55–62, https://doi.org/10.1117/12.2293584.

[28] A. Diaz-Pinto, S. Morales, V. Naranjo, T. Köhler, J. M. Mossi, and A. Navea, "CNNs for automatic glaucoma assessment using fundus images: an extensive validation," *BioMedical Engineering OnLine*, vol. 18, no. 1, Mar. 2019, Art. no. 29, https://doi.org/10.1186/s12938-019-0649-y.

[29] J. I. Orlando *et al.*, "REFUGE Challenge: A unified framework for evaluating automated methods for glaucoma assessment from fundus photographs," *Medical Image Analysis*, vol. 59, Jan. 2020, Art. no. 101570, https://doi.org/10.1016/j.media.2019.101570.

[30] J. Staal, M. D. Abramoff, M. Niemeijer, M. A. Viergever, and B. van Ginneken, "Ridge-based vessel segmentation in color images of the retina," *IEEE Transactions on Medical Imaging*, vol. 23, no. 4, pp. 501–509, Apr. 2004, https://doi.org/10.1109/TMI.2004.825627.

[31] E. Decencière *et al.*, "Feedback on a Publicly Distributed Image Database: The Messidor Database," *Image Analysis and Stereology*, vol. 33, no. 3, pp. 231–234, Aug. 2014, https://doi.org/10.5566/ias.1155.

[32] C. de Vente *et al.*, "AIROGS: Artificial Intelligence for Robust Glaucoma Screening Challenge," *IEEE Transactions on Medical Imaging*, vol. 43, no. 1, pp. 542–557, Jan. 2024, https://doi.org/10.1109/TMI.2023.3313786.

[33] L. K. Singh, M. Khanna, S. Thawkar, and R. Singh, "Nature-inspired computing and machine learning based classification approach for glaucoma in retinal fundus images," *Multimedia Tools and Applications*, vol. 82, no. 27, pp. 42851–42899, Nov. 2023, https://doi.org/10.1007/s11042-023-15175-6.

[34] J.-H. Wu, T. Nishida, R. N. Weinreb, and J.-W. Lin, "Performances of Machine Learning in Detecting Glaucoma Using Fundus and Retinal Optical Coherence Tomography Images: A Meta-Analysis," *American Journal of Ophthalmology*, vol. 237, pp. 1–12, May 2022, https://doi.org/10.1016/j.ajo.2021.12.008.

[35] G. Suguna and R. Lavanya, "Performance Assessment of EyeNet Model in Glaucoma Diagnosis," *Pattern Recognition and Image Analysis*, vol. 31, no. 2, pp. 334–344, Apr. 2021, https://doi.org/10.1134/S1054661821020164.